HHS Public Access

Author manuscript

Nat Cell Biol. Author manuscript; available in PMC 2013 January 01.

Published in final edited form as:

Nat Cell Biol. ; 14(7): 707–716. doi:10.1038/ncb2523.

ER network formation requires a balance of the dynamin-like GTPase Sey1p and Lnp1p, a member of the Lunapark family

Shuliang Chen[1,2], **Peter Novick**[1,#], and **Susan Ferro-Novick**[1,2,#]

[1]Department of Cellular and Molecular Medicine, University of California at San Diego, La Jolla, CA 92093-0668

[2]Howard Hughes Medical Institute, University of California at San Diego, La Jolla, CA 92093-0668

Abstract

While studies on endoplasmic reticulum (ER) structure and dynamics have focused on the ER tubule forming proteins (reticulons and DP1/Yop1p) and the tubule fusion protein atlastin, nothing is known about the proteins and processes that act to counter-balance this machinery. Here we show that Lnp1p, a member of the conserved lunapark family, plays a role in ER network formation. Lnp1p binds to the reticulons and Yop1p and resides at ER tubule junctions in both yeast and mammalian cells. In the yeast *Saccharomyces cerevisiae*, the interaction of Lnp1p with the reticulon protein, Rtn1p, and the localization of Lnp1p to ER junctions are regulated by Sey1p, the yeast ortholog of atlastin. We propose that Lnp1p and Sey1p act antagonistically to balance polygonal network formation. In support of this proposal, we show that the collapsed, densely reticulated ER network in *lnp1*Δ cells is partially restored when the GTPase activity of Sey1p is abrogated.

Introduction

The ER possesses a unique and highly conserved morphology that reflects the many essential roles it plays in all eukaryotic cells [1, 2]. Within each cell, it typically forms one contiguous structure of interconnected sheets and tubules arranged into a polygonal network that makes numerous connections with the outer membrane of the nuclear envelope. This network is spread throughout the cell, all the way to its cortex, by a dynamic process of tubule extension and tubule fusion, leading to the formation of new polygons. At steady state, polygon formation is balanced by ring closure; the sliding of an ER junction along the side of a polygon until ultimately the polygon is lost [3].

ER tubules and networks are generated and stabilized by the reticulons, DP1/Yop1p and atlastin. These components are conserved throughout evolution [2, 4–6]. The reticulons are

[#]Correspondence should be addressed to: Dr. Susan Ferro-Novick, Department of Cellular and Molecular Medicine, University of California at San Diego, Howard Hughes Medical Institute, George Palade Labs, room 315, Phone: (858) 246-0466, Fax: (858) 534-7688, sfnovick@ucsd.edu. Dr. Peter Novick, Department of Cellular and Molecular Medicine, University of California at San Diego, George Palade Labs, room 233A, Phone: (858) 246-0465, Fax: (858) 534-7688, pnovick@ucsd.edu.

transmembrane proteins [2, 4] that work synergistically with the reticulon interacting protein, DP1/Yop1p, to add positive curvature to the bilayer of the ER membrane [2, 4, 7]. Consistent with this role, these proteins are concentrated on tubular elements of the ER and the highly curved edges of ER sheets [2, 4, 8]. The dynamin-like GTPase atlastin binds to the reticulons and DP1/Yop1p and promotes ER tubule fusion. It localizes to the three-way junctions that interconnect the tubular elements of the ER to form the ER network [6, 9, 10]. In humans, mutations in either atlastin-1 or REEP1, a member of the DP1/Yop1p protein family [2], lead to a distal axonopathy of corticospinal neurons [11, 12]. However, when orthologs of the reticulons, DP1/Yop1p and atlastin are all disrupted in the same haploid yeast strain, growth is not affected. These observations suggest that neurons, which are highly elongated, may be particularly sensitive to defects in ER morphogenesis.

In this study, we report that a member of the conserved lunapark protein family [13], Lnp1p, defined by two transmembrane domains and a zinc finger motif, is required for ER network formation. Lnp1p works in synergy with the reticulons and Yop1p, but in antagonism to Sey1p (yeast ortholog of atlastin). It resides at three-way ER tubule junctions in both yeast and mammalian cells and it interacts with the reticulons, Yop1p and Sey1p. Sey1p negatively regulates the interaction of Lnp1p with the reticulons and is necessary for the localization of Lnp1p to ER junctions. We propose that Lnp1p counterbalances Sey1p-directed polygon formation by promoting polygon loss through ring closure.

Results

Lnp1p is required to maintain the cortical ER network and localizes to ER tubule junctions

To identify novel components of the machinery required to generate the cortical ER network in yeast, we screened the *Saccharomyces cerevisiae* deletion library using Rtn1p fused to GFP (Rtn1p-GFP) as a marker for the ER. There are two genes in yeast encoding reticulons, *RTN1* and *RTN2*. Rtn1p is very abundant, while Rtn2p is only expressed in the presence of high salt [2, 4] (www.yeastgenome.org). The advantage of using Rtn1p-GFP is that it is much brighter than the other markers that have previously been used to study the cortical ER network in yeast [14–16] and it specifically labels the tubular ER, as well as the edges of ER sheets [2, 4, 8, 17]. The screen we employed led to the identification of four ORFs (*SCS2*, *PHO85*, *CHO1* and *YHR192W*) whose loss disrupts the cortical ER network in yeast (Fig. S1a). Of these ORFs, only *SCS2* and *YHR192W* encode integral ER membrane proteins. The role of Scs2p in ER structure and inheritance has previously been reported [18]. Here we focus on *YHR192W*. For subsequent studies we disrupted this ORF in our strain background. When two different ER markers (Rtn1p-RFP and Sec61p-GFP) were used to analyze the ER in a strain deleted for *YHR192W*, the morphology was found to be abnormal in approximately 91% of the mutant cells (Fig. 1a, left and right). Large sectors of the cortex lacking cortical ER were observed and regions where the ER network appeared to have collapsed were also seen in the mutant (Fig. 1a and 1c, left). A blast search of YHR192W revealed it to be the sole yeast member of a conserved protein family named Lunapark [13]. This protein family is defined by the presence of two N-terminal predicted transmembrane domains and a C-terminal zinc finger motif (Fig. 1b). Adjacent to the zinc finger, in animal homologues, is the sequence LNPARK, hence the gene name *LNP1*(LNPARK).

An *lnp1* mutant (*lnp1-1*), in which the four cysteine residues of the zinc finger (Fig. 1b, blue) were mutated to alanine, exhibited the same ER phenotype as *lnp1*Δ, indicating a functional role for this motif (Fig. 1c). To examine the consequences of disrupting this motif in more detail, we constructed strains that contain one (*lnp1-5*, C223A), two (*lnp1-2*, C223A C226A) and four (*lnp1-1*, C223A C226A C244A C247A) cysteine mutations in the zinc finger motif. Interestingly, the ER morphology became increasingly more aberrant as the number of cysteine mutations increased (Fig. 2a; Fig. S1b and S1c). Large cortical sectors devoid of ER appeared and the polygons became smaller on average with each additional mutation until they could no longer be resolved by light microscopy. These findings suggest that the ER became more densely reticulated with each mutation in Lnp1p. Thin section electron microscopy revealed short sections of ER between small, closely spaced openings in *lnp1*Δ cells (Fig. 3), confirming that the ER was densely reticulated in the mutant.

Next, we performed colocalization studies with Lnp1p-3xGFP and the ER marker proteins Rtn1p-RFP, Sey1p-5xRFP and the ER retrieval sequence HDEL fused to DsRed. This analysis revealed that Lnp1p-3xGFP specifically resides on puncta that line the tubular ER (Fig. 2b), and at junctions where the tubular ER meets the nuclear envelope (Fig. S2a). When we deconvolved an area of the ER at the periphery of the cell using Openlab software, we were able to resolve the polygonal network marked by Rtn1p-GFP (Fig. 2c, middle bottom panel). Lnp1p-3xGFP was found at the three-way junctions of the ER network (Fig. 2c, bottom), partially overlapping or adjacent to Sey1p-5xRFP (Fig. 2d). In mammalian cells, Lnp1 also localized to the three way junctions of the ER (Fig. 2e), suggesting that its function is conserved from yeast to higher cells. Interestingly, in the absence of Lnp1p, the ER junctions were no longer clearly resolved and Sey1p-5xRFP appeared to spread throughout the densely reticulated ER network (Fig. S2b).

Lnp1p acts in synergy with Rtn1p, but in antagonism to Sey1p

To begin to address the relationship of Lnp1p to the reticulons and Yop1p, we disrupted *LNP1* in strains that lacked the reticulons and/or Yop1p. When we disrupted *RTN1* in haploid cells that were also disrupted for *LNP1*, we observed a growth defect (Fig. 4a, left panel, see white circles and doubling times in Fig.S3a). This growth defect was further enhanced when *YOP1* was deleted in the *lnp1*Δ*rtn1*Δ mutant (Fig. 4a, middle panel, see white squares; Fig. S3a), and was most dramatic when *LNP1* was disrupted in a strain that lacked both reticulon genes (*RTN1* and *RTN2*) and *YOP1* (Fig. 4a, right panel, see white triangles; Fig. S3a). No growth defect was observed when *lnp1*Δ was deleted in combination with *rtn2*Δ, *yop1*Δ or an *rtn2*Δ *yop1*Δ double deletion (Fig. S3a). Thus, the enhancement of the growth defect appears to be dependent on the loss of Rtn1p. Consistent with these genetic studies, we observed an enhancement of the cortical ER defect in *lnp1*Δ*rtn1*Δ, *lnp1*Δ*rtn1*Δ*yop1*Δ and *lnp1*Δ*rtn1*Δ*rtn2*Δ*yop1*Δ mutant cells (Fig. 4b). As previously reported [2], disrupting *YOP1* in mutant cells that lacked one or both reticulon genes also enhanced the cortical ER defect (Fig. 4b), however, no growth defect was associated with this phenotype (Fig. 4c). Together these findings indicate that Lnp1p acts in synergy with Rtn1p to structure the cortical ER.

To address if Lnp1p and Sey1p act in synergy, we deleted *SEY1* in the *lnp1*Δ*rtn1*Δ double, *lnp1*Δ*rtn1*Δ*yop1*Δ triple and *lnp1*Δ*rtn1*Δ*rtn2*Δ*yop1*Δ quadruple mutants. To our surprise, we found that the loss of Sey1p strongly suppressed the growth defects of each of these mutants (Fig. 4c, boxed area). These genetic findings indicate that Lnp1p acts in antagonism to Sey1p. Additionally, although the ER network appeared to be less branched in the *sey1*Δ mutant (Fig. 4d, Fig. S3b), disruption of *SEY1*Δ largely restored the collapsed, more highly branched network in the *lnp1*Δ mutant (Fig. 4d, Fig. S3b) in over 70% of the cells examined (Fig. 4e). The loss of GTPase activity is sufficient for suppression, as a *sey1* mutant defective in GTP-binding (*sey1*^{K50A}), suppressed the cortical ER defect in the *lnp1*Δ mutant as efficiently as *sey1*Δ (Fig. 4d and 4e). Deletion of *SEY1* also partially rescued the cortical ER defect in the *lnp1*Δ*rtn1*Δ, *lnp1*Δ*rtn1*Δ*yop1*Δ and *lnp1*Δ*rtn1*Δ*rtn2*Δ*yop1*Δ mutants (Fig. S3c).

Sey1p-GTP restricts Lnp1p to ER tubule junctions

To address how Sey1p acts in antagonism to Lnp1p, we examined the localization of Lnp1p-3xGFP in the *sey1*Δ and *sey1*^{K50A} mutants. Interestingly, Lnp1p-3xGFP was no longer restricted to puncta on the cortical ER in these mutants (Fig. 5a, middle and bottom panel). Instead, similar to Sec61p-2xRFP and DsRed-HDEL, Lnp1p-3xGFP was spread evenly throughout both the cortical ER and nuclear envelope (Fig. 5a; Fig. S2a). Quantitation of the phenotype revealed that Lnp1p-3xGFP was spread throughout the ER in the majority of the *sey1*Δ and *sey1*^{K50A} cells examined (Fig. 5b). Unlike Lnp1p, the localization of Rtn1p-RFP and Yop1p-RFP was unaltered in the *sey1*Δ mutant (Fig. S4a,b). A closer examination of the peripheral ER network in both the *sey1*Δ and *sey1*^{K50A} mutants revealed that Lnp1p-3xGFP was in the ER sheets and not the ER tubule junctions (Fig. 5c). Interestingly, while Lnp1p-3xGFP was in the sheets, Rtn1p-GFP lined the more highly curved edges of the sheets in these mutants. Together these findings indicate that, unlike the reticulons and Yop1p, Lnp1p does not have an intrinsic ability to localize to highly curved membrane domains (Fig. 5c). Additionally, these findings show that Sey1p-GTP appears to play an important role in restricting Lnp1p to ER tubule junctions.

The interaction of Lnp1p with Rtn1p is regulated by Sey1p

The observation that Lnp1p acts in synergy with Rtn1p and in antagonism to Sey1p suggests that Lnp1p might physically interact with Rtn1p and/or Sey1p. To begin to address this possibility, we performed immunoprecipitation experiments. Lysates prepared from three different strains containing Lnp1p-3xHA with either Rtn1p-3xFLAG, Sey1p-3xFLAG, or the Rtn1p interacting protein Yop1p (tagged with 3xFLAG) were incubated with anti-HA affinity matrix. The beads were then washed and blotted with anti-FLAG antibody. This analysis revealed that Lnp1p-3xHA specifically interacts with all three proteins, but not with Sec22p, a type II membrane protein that resides on the ER and Golgi [19](Fig. 6a). The interaction was dependent on the presence of the HA tag as no Rtn1p-3xFLAG, Sey1p-3xFLAG or Yop1p-3xFLAG was detected in the precipitate when lysate containing untagged Lnp1p was incubated with anti-HA affinity matrix (Fig. S4c). The amount of Rtn1p that co-precipitated with Lnp1p was similar to the amount of Sey1p that co-precipitated with Rtn1p (Fig. S4d).

To determine if Sey1p regulates the interaction of Lnp1p with the reticulons, we examined the interaction of Lnp1p-3xHA with Rtn1p-3xFLAG in strains in which *SEY1* was either deleted or overexpressed from the inducible *GAL1* promoter. Interestingly, we precipitated more Rtn1p with Lnp1p when *SEY1* was deleted (Fig. 6b, compare lanes 1 and 2), and less Rtn1p with Lnp1p when Sey1p was overexpressed (Fig. 6b, compare lanes 3 and 4). Thus, Sey1p appears to negatively regulate the interaction of Lnp1p with Rtn1p. When we examined the consequences of overexpressing Sey1p on its localization and on the localization of Rtn1p, Yop1p and Lnp1p, we found that Sey1p forms large round structures that predominantly reside at the periphery of the cell (Fig. S5). These structures also contained Rtn1p and Yop1p (Fig. S5d and S5e), but not Lnp1p (Fig. S5a-c), consistent with the observation that less Rtn1p is precipitated with Lnp1p when Sey1p is overexpressed (Fig. 6b). EM analysis demonstrated that the large structures consist of tubular membranes (Fig. S5f). These tubular membranes were not present when Lnp1p was overexpressed from the inducible *GAL1* promoter (Fig. S5g). Lnp1p was found on the tubular ER and nuclear envelope within 2 hr after induction (Fig. S6a). After 4 hr, the nuclear envelope and cortical ER became aberrant and the localization of Rtn1p and Lnp1p no longer overlapped (Fig. S6a; S6b). Eventually, the overproduction of Lnp1p led to cell death (Fig. S6e). Interestingly, this growth defect was suppressed when Lnp1p was overexpressed in a strain that also overexpressed Sey1p (Fig. S6d and S6e). Under conditions of co-overexpression, Lnp1p-GFP and Sey1p-RFP were found to co-localize in large, round peripheral structures. (Fig. S6c).

Sey1p, but not Lnp1p, is defective in cortical ER and nuclear ER fusion

Atlastin, but not its putative homologue Sey1p, has been directly shown to promote the fusion of ER membranes [9]. As Sey1p and Lnp1p appear to have opposing effects, we wanted to address if the loss of Lnp1p suppresses the presumed fusion defect in the *sey1*Δ mutant. To do this, we established an assay that measures ER-ER fusion in vivo during the mating reaction.

Yeast cells have two mating types, MAT*a* and MAT*α*. When cells of the opposite mating type come in contact with each other, in response to pheromone signaling, the wall at the contact site of each cell is degraded (cell wall remodeling) and the plasma membranes of the two cells fuse (Fig. 7a). This allows the ER in the two parent cells to fuse, mixing their lumenal contents, and the nuclei from each cell to fuse forming a zygote [20]. To assess cortical ER-ER fusion, we mated one cell expressing the ER lumenal marker DsRed-HDEL with another cell expressing cytosolic GFP (Fig. S7). The time at which the plasma membranes fused, as indicated by the transfer of cytosolic GFP between the two parent cells, was defined as T=0 (Fig. 7a). We then measured the time it took to initiate and complete ER lumenal mixing in wild type, *lnp1*Δ, *sey1*Δ and *lnp1*Δ*sey1*Δ cells (Fig. S7). This analysis revealed that the start (Fig. 7b) and completion (Fig. 7c) of ER mixing was similar in wild type and *lnp1*Δ cells. Mixing, however, was delayed in the *sey1*Δ mutant. This delay was not significantly suppressed in an *lnp1*Δ*sey1*Δ double mutant. Consistent with the hypothesis that Sey1p mediates ER fusion at the contact zone where the two cells fuse, we found that Sey1p-5xRFP localizes to this zone in wild type zygotes (Fig. S8, top), while Lnp1p (Fig. S8, middle) and Rtn1p (Fig. S8, bottom) do not.

We also assessed nuclear envelope fusion in the strains described above by mixing MAT*a* and MATα cells that expressed Sec61p-GFP. The cell suspension was plated on a YPD plate for 4 hr at 25°C, and the zygotes that formed a new bud near the site of cell fusion were analyzed further (Fig. 8a). The mating pairs with unfused nuclei (three versus two nuclei) and the fraction that failed to go on to form diploid cells (Fig. 8b and 8c) were measured. Cells were determined to be diploid if they were able to sporulate and failed to mate with either MAT*a* or MATα tester strains. This analysis revealed that Sey1p, but not Lnp1p, is required for nuclear fusion, i.e. *sey1*Δ is defective in karyogamy. Thus Sey1p is required for both cortical ER-ER and nuclear ER fusion. Additionally, similar to the ER-ER fusion defect, the nuclear fusion defect of the *sey1*Δ mutant was not strongly suppressed in the *sey1*Δ *lnp1*Δ double mutant. Therefore, Lnp1p does not appear to antagonize Sey1p by inhibiting a Sey1p-independent ER fusion pathway.

Discussion

The ER is shaped through the addition of bilayer curvature by the reticulons and DP1/Yop1p [2, 4, 21]. Curiously, although the reticulons and DP1/Yop1p are sufficient for the formation of tubules in vitro [5], the simultaneous loss of Rtn1p, Rtn2p and Yop1p does not lead to an appreciable growth defect in yeast. ER tubule interconnections are formed when the dynamin-like GTPase atlastin fuses ER tubules to each other to form a network [6]. Currently, it is unknown if atlastin is sufficient for forming ER tubular junctions, however, in its absence long unbranched tubules predominate [6]. In yeast, the atlastin homologue Sey1p facilitates homotypic ER-ER and nuclear ER envelope fusion during the mating reaction. Additional, as yet unidentified components must be needed for ER network formation, as yeast cells lacking Sey1p, the reticulons and Yop1p are not impaired for growth.

Here we show that a member of a conserved protein family, named Lunapark, is a player in ER network formation. Interestingly, like mutations in the Sey1p homologue atlastin or the Yop1p homolog REEP1, the *lnp-1* mutant of *C. elegans* has been linked to neuronal defects [22]. In yeast, the loss of Lnp1p in an *rtn1*Δ*rtn2*Δ*yop1*Δ triple mutant leads to a striking growth defect and profound ER morphology defects, indicating that Lnp1p acts in synergy with the reticulons and Yop1p to structure the ER. Lnp1p contains two transmembrane domains and a zinc finger motif that is essential for its function. It interacts with Rtn1p, Yop1p and Sey1p and localizes to ER junctions where it partially overlaps with, or is adjacent to, Sey1p. The localization of Lnp1p to ER junctions is dependent on Sey1p-GTP, which also negatively regulates the interaction of Lnp1p with Rtn1p.

The synergistic genetic interactions between *LNP1* and *RTN1* could indicate that Lnp1p and Rtn1p either have redundant functions, or they act on converging pathways. It seems unlikely that Rtn1p acts redundantly with Lnp1p since it is at least ten times more abundant than Lnp1p (www.yeastgenome.org) and it localizes to the tubular ER and the edges of ER sheets [2, 4, 8], while Lnp1p resides at ER junctions. Furthermore, the phenotypes of *lnp1*Δ and *rtn1*Δ mutants, as revealed by electron microscopy, are distinct. Loss of Lnp1p leads to the formation of densely reticulated ER, while the loss of Rtn1p results in non-fenestrated sheets [4].

The strong suppression by *sey1*Δ of the growth defects of the *lnp1*Δ*rtn1*Δ, *lnp1*Δ*rtn1*Δ*yop1*Δ *and lnp1*Δ*rtn1*Δ*rtn2*Δ*yop1*Δ mutants suggests that Lnp1p balances the function of Sey1p. Furthermore, the suppression of the ER morphology defects of *lnp1*Δ by *sey1*Δ indicates that this balance is important in forming a normal ER network. One possible role for Lnp1p is to balance the fusion activity of Sey1p by mediating ER fission. A balance of fission and fusion events is required to maintain normal mitochondrial morphology [23]. The dynamin-like GTPase Dnm1p, promotes mitochondrial fission [24], which balances the mitochondrial fusion activity of Fzo1p, an outer mitochondrial membrane GTPase [25, 26]. Unlike Dnm1p, Lnp1p is not a GTPase and fission of ER tubules has not been directly observed by live cell imaging. Alternatively, Lnp1p could also balance Sey1p function by directing ER polygon loss through ring closure. Lnp1p might be needed for the sliding of a three-way junction along an ER tubule to allow a polygon to shrink or perhaps for the final membrane scission event needed to resolve the residual hole, completing the process of ring closure. In either case, the loss of Lnp1p would be predicted to result in the accumulation of excess polygons of decreasing size. The densely reticulated cortical ER observed by electron microscopy in the *lnp1*Δ mutant is consistent with this proposal.

Methods

Screen of the yeast deletion library

The MAT *a* deletion collection (derivative of BY4741, Open Biosystems) was screened in 96-well plates for defects in ER morphology. Briefly, an aliquot (1 μl) of each strain was transferred into 100 μl of YPD medium supplemented with G418 (200 μg/ml) and incubated for 2–3 days at 25°C. This step was repeated three times before the cells were screened. To screen the cells, all strains were grown in 100 μl of YPD medium for 24 hr at 25°C. Subsequent to this incubation, the cells were centrifuged for 5 min at 3000 rpm, and the pellet was re-suspended in 20 μl of transformation buffer (0.2 M LiAc, 40% PEG 3350, 100 mM DTT, pH 7.5) containing 10 μg of carrier DNA (salmon sperm) and 100 ng of plasmid DNA (pRS315-RTN1-GFP). The cells were then incubated at 42°C for 30 min and the transformation buffer was removed by centrifugation. The transformants were selected in 150 μl of SC-Leu media. The transformed strain (1 μl) was inoculated into 100 μl of fresh SC-Leu media and incubated at 25°C for 12 hr. The morphology of the cortical ER, marked by Rtn1p-GFP, was examined by fluorescence microscopy.

Fluorescence microscopy

Yeast cells (see Table S1) were grown at 25°C to early log phase (OD_{600} = 0.3–0.6). Approximately 5 OD_{600} units of cells were pelleted at 3000 rpm, resuspended in 250 μl of ice-cold growth medium and examined on a Axio Imager Z1 fluorescence microscope using a 100x oil-immersion objective. Images were captured with an Axio Cam MRm digital camera and AxioVision software, and deconvolved using OpenLab software.

Electron microscopy

Yeast cells were grown overnight to early log phase (OD_{600}=0.3–0.6) at 25°C. Approximately 10 OD_{600} units of cells were harvested using a 0.22 μm filter apparatus, washed with 10 ml of 0.1 M cacodylate (pH 6.8), resuspended in 10 ml of fixative (0.1 M

cacodylate, 4% glutaraldehyde, pH 6.8) and incubated for 1 hr at room temperature before the cells were stored overnight at 4°C. The next day, the fixed cells were washed with 50 mM KPi (pH 7.5) and then incubated at 37°C for 40 min with buffer containing Zymolase 100T (0.25 mg/ml). After the incubation, the cells were washed with ice cold 0.1 M cacodylate buffer, incubated in 2% OsO_4 for 1 hr on ice, washed with water and then incubated in 2% uranyl acetate (UrAc) for 1 hr at room temperature. Samples were dehydrated using a series of ethanol washes, and incubated overnight in Spurr resin. Samples were embedded in fresh Spurr resin, and baked at 80°C for at least 24 hr. Sections were stained with lead citrate and UrAc and images were acquired using a Tecnai G^2 Spirit transmission electron microscope equipped with a Gatan Ultra Scan 4000 CCD camera.

Mammalian cell culture, transfection and confocal microscopy

COS-7 cells were grown at 37°C in a 5% CO_2 incubator in Dulbecco's MEM with high glucose and 10% fetal bovine serum. To construct Lnp1-GFP, human Lnp1 was PCR-amplified from a human cDNA clone (Open Biosystems, NCBI accession number: BC105132), and inserted into pAcGFP1-N1 using the SacI/SacII restriction sites. Transfection of plasmid DNA (pAc-Rtn4b-mCherry and pAc-Lnp1-GFP) into COS-7 cells was performed using Lipofectamine 2000 (Invitrogen). Cells were imaged using an Olympus FV1000 confocal laser scanning microscope and FluoView software.

Immunoprecipitation protocol

Yeast cells grown to an OD_{600}=1.0 were harvested by centrifugation, washed once with ice-cold water and resuspended in spheroplasting buffer (1.4 M sorbitol, 50 mM NaPi (pH 7.4), 50 mM 2-mercaptoethanol, 10μg/OD_{600} Zymolyase-100T). The resuspended cells were incubated at 37°C for 30 min with gentle shaking, pelleted through a chilled sorbitol cushion (1.7 M sorbitol, 20 mM HEPES, pH 7.4), and the pellet was resuspended in lysis buffer (25 mM HEPES, 150 mM KCl, 5 mM $MgCl_2$, 1 mM DTT, 1 mM PMSF, 1x protease inhibitor [27], 1% Digitonin, pH 7.4) using a dounce homogenizer (40 strokes). The lysate was centrifuged at 37,000 × g for 20 min at 4°C, and the protein concentration of the supernatant was measured using the Bradford assay.

The protein concentration of the lysate was adjusted to 2–4 mg/ml with lysis buffer, and 0.5–1.0 ml of the lysate was incubated overnight at 4°C with 10–20 μl of anti-HA affinity matrix (Clone 3F10, Roche). The matrix was pelleted at 5000 rpm for 30 sec, and washed three times with 1 ml of cold lysis buffer that contained 0.2% digitonin. The matrix was heated to 100°C in sample buffer (62.5 mM Tris-HCl, 2% SDS, 5% 2-mercaptoethanol, 10% glycerol, 0.002% bromophenol, pH 6.8) for 5 min. The eluted protein was subjected to SDS-PAGE and immunoblotted with anti-HA (1:2000 dilution, Clone HA.11, Covance, MMS-101R), anti-FLAG (1:2000 dilution, Clone M2, Sigma, F 1804) and anti-Sec22p (1:1000 dilution) antibodies. The secondary antibodies used were goat anti-mouse IgG-HRP (1:10,000 dilution, Promega, W402B) or donkey anti-rabbit IgG-HRP (1:10,000 dilution, GE Healthcare, NA9340V).

Time-lapse imaging of cortical ER fusion

Haploid MAT*a* and MATα cells were grown to log phase at 25°C in SC media. Five hundred μl of each cell culture were mixed and then centrifuged at 3000 rpm. To prepare a slide of the mating mix, the cell pellet was resuspended in 10 μl of fresh SC media, and applied to a 1.5-mm-thick pad of 3% low temperature agarose prepared in SC medium. A coverslip was then applied to the sample, sealed with vaseline and incubated at 25°C for 45–60 min. Cell fusion was examined at 25°C on a Axio Imager Z1 fluorescence microscope using a 63x oil-immersion objective. Images were captured with an Axio Cam MRm digital camera and AxioVision software, and deconvolved using OpenLab software.

Zygote formation assay

Haploid MAT*a* and MATα cells grown to early stationary phase at 25°C were harvested by centrifugation at 3000 rpm. The cells were resuspended in fresh YPD media (OD_{600}=8.0) and incubated at 25°C with shaking for 30 min. MAT*a* cells (3 μl) were mixed with an equal volume of MATα cells and plated onto a fresh YPD plate that was incubated at 25°C for 2–4 hr. Cell fusion and zygote formation was then assessed under the microscope. To measure the efficiency of diploid formation, zygotes were picked with a dissection needle and transferred to a YPD plate that was incubated for 4 days at 25°C. Cells were scored as diploid if they were able to sporulate and could not mate with either MAT*a* or MATα tester strains.

Statistical Analysis

P values were calculated using the Student's t-test. The statistical significance reported is from independent experiments and presented as mean values. The error bars in the Figure legends represent standard deviation (S.D.) or standard error of the mean (S.E.M.) as specified in the legends.

Supplementary Material

Refer to Web version on PubMed Central for supplementary material.

Acknowledgments

We thank Dr. Gia Voeltz for plasmids. We also thank Ying Jones in the Electron Microscopy Facility in the Department of Cellular and Molecular Medicine at the University of California at San Diego, headed by Dr. Marilyn Farquhar, for the preparation of EM samples, and we acknowledge use of the UCSD Neuroscience Microscopy Facility funded by grant P30 NS047101. This work was supported by a grant from the National Institutes of Health (GM073892) and the Howard Hughes Medical Institute. Salary support for S.C. and SF-N was provided by the Howard Hughes Medical Institute.

References

1. Du Y, Ferro-Novick S, Novick P. Dynamics and inheritance of the endoplasmic reticulum. J Cell Sci. 2004; 117:2871–2878. [PubMed: 15197242]
2. Voeltz GK, Prinz WA, Shibata Y, Rist JM, Rapoport TA. A class of membrane proteins shaping the tubular endoplasmic reticulum. Cell. 2006; 124:573–586. [PubMed: 16469703]
3. Lee C, Chen LB. Dynamic behavior of endoplasmic reticulum in living cells. Cell. 1988; 54:37–46. [PubMed: 3383243]

4. De Craene JO, et al. Rtn1p is involved in structuring the cortical endoplasmic reticulum. Mol Biol Cell. 2006; 17:3009–3020. [PubMed: 16624861]
5. Hu J, et al. Membrane proteins of the endoplasmic reticulum induce high-curvature tubules. Science. 2008; 319:1247–1250. [PubMed: 18309084]
6. Hu J, et al. A class of dynamin-like GTPases involved in the generation of the tubular ER network. Cell. 2009; 138:549–561. [PubMed: 19665976]
7. West M, Zurek N, Hoenger A, Voeltz GK. A 3D analysis of yeast ER structure reveals how ER domains are organized by membrane curvature. J Cell Biol. 2011; 193:333–346. [PubMed: 21502358]
8. Schuck S, Prinz WA, Thorn KS, Voss C, Walter P. Membrane expansion alleviates endoplasmic reticulum stress independently of the unfolded protein response. J Cell Biol. 2009; 187:525–536. [PubMed: 19948500]
9. Orso G, et al. Homotypic fusion of ER membranes requires the dynamin-like GTPase atlastin. Nature. 2009; 460:978–983. [PubMed: 19633650]
10. Park SH, Zhu PP, Parker RL, Blackstone C. Hereditary spastic paraplegia proteins REEP1, spastin, and atlastin-1 coordinate microtubule interactions with the tubular ER network. J Clin Invest. 2010; 120:1097–1110. [PubMed: 20200447]
11. Beetz C, et al. REEP1 mutation spectrum and genotype/phenotype correlation in hereditary spastic paraplegia type 31. Brain. 2008; 131:1078–1086. [PubMed: 18321925]
12. Salinas S, Proukakis C, Crosby A, Warner TT. Hereditary spastic paraplegia: clinical features and pathogenetic mechanisms. Lancet Neurol. 2008; 7:1127–1138. [PubMed: 19007737]
13. Spitz F, Gonzalez F, Duboule D. A global control region defines a chromosomal regulatory landscape containing the HoxD cluster. Cell. 2003; 113:405–417. [PubMed: 12732147]
14. Du Y, Pypaert M, Novick P, Ferro-Novick S. Aux1p/Swa2p is required for cortical endoplasmic reticulum inheritance in Saccharomyces cerevisiae. Mol Biol Cell. 2001; 12:2614–2628. [PubMed: 11553703]
15. Estrada P, et al. Myo4p and She3p are required for cortical ER inheritance in Saccharomyces cerevisiae. J Cell Biol. 2003; 163:1255–1266. [PubMed: 14691136]
16. Prinz WA, et al. Mutants affecting the structure of the cortical endoplasmic reticulum in Saccharomyces cerevisiae. J Cell Biol. 2000; 150:461–474. [PubMed: 10931860]
17. Shibata Y, et al. Mechanisms determining the morphology of the peripheral ER. Cell. 2010; 143:774–788. [PubMed: 21111237]
18. Loewen CJ, Young BP, Tavassoli S, Levine TP. Inheritance of cortical ER in yeast is required for normal septin organization. J Cell Biol. 2007; 179:467–483. [PubMed: 17984322]
19. Barrowman J, Sacher M, Ferro-Novick S. TRAPP stably associates with the Golgi and is required for vesicle docking. Embo J. 2000; 19:862–869. [PubMed: 10698928]
20. Grote E. Cell fusion assays for yeast mating pairs. Methods Mol Biol. 2008; 475:165–196. [PubMed: 18979244]
21. Moss TJ, Andreazza C, Verma A, Daga A, McNew JA. Membrane fusion by the GTPase atlastin requires a conserved C-terminal cytoplasmic tail and dimerization through the middle domain. Proc Natl Acad Sci U S A. 2011; 108:11133–11138. [PubMed: 21690399]
22. Ghila L, Gomez M. The evolutionarily conserved gene LNP-1 is required for synaptic vesicle trafficking and synaptic transmission. Eur J Neurosci. 2008; 27:621–630. [PubMed: 18279315]
23. Hoppins S, Lackner L, Nunnari J. The machines that divide and fuse mitochondria. Annu Rev Biochem. 2007; 76:751–780. [PubMed: 17362197]
24. Bleazard W, et al. The dynamin-related GTPase Dnm1 regulates mitochondrial fission in yeast. Nat Cell Biol. 1999; 1:298–304. [PubMed: 10559943]
25. Hales KG, Fuller MT. Developmentally regulated mitochondrial fusion mediated by a conserved, novel, predicted GTPase. Cell. 1997; 90:121–129. [PubMed: 9230308]
26. Hermann GJ, et al. Mitochondrial fusion in yeast requires the transmembrane GTPase Fzo1p. J Cell Biol. 1998; 143:359–373. [PubMed: 9786948]

27. Ruohola H, Kabcenell AK, Ferro-Novick S. Reconstitution of protein transport from the endoplasmic reticulum to the Golgi complex in yeast: the acceptor Golgi compartment is defective in the sec23 mutant. J Cell Biol. 1988; 107:1465–1476. [PubMed: 3049622]

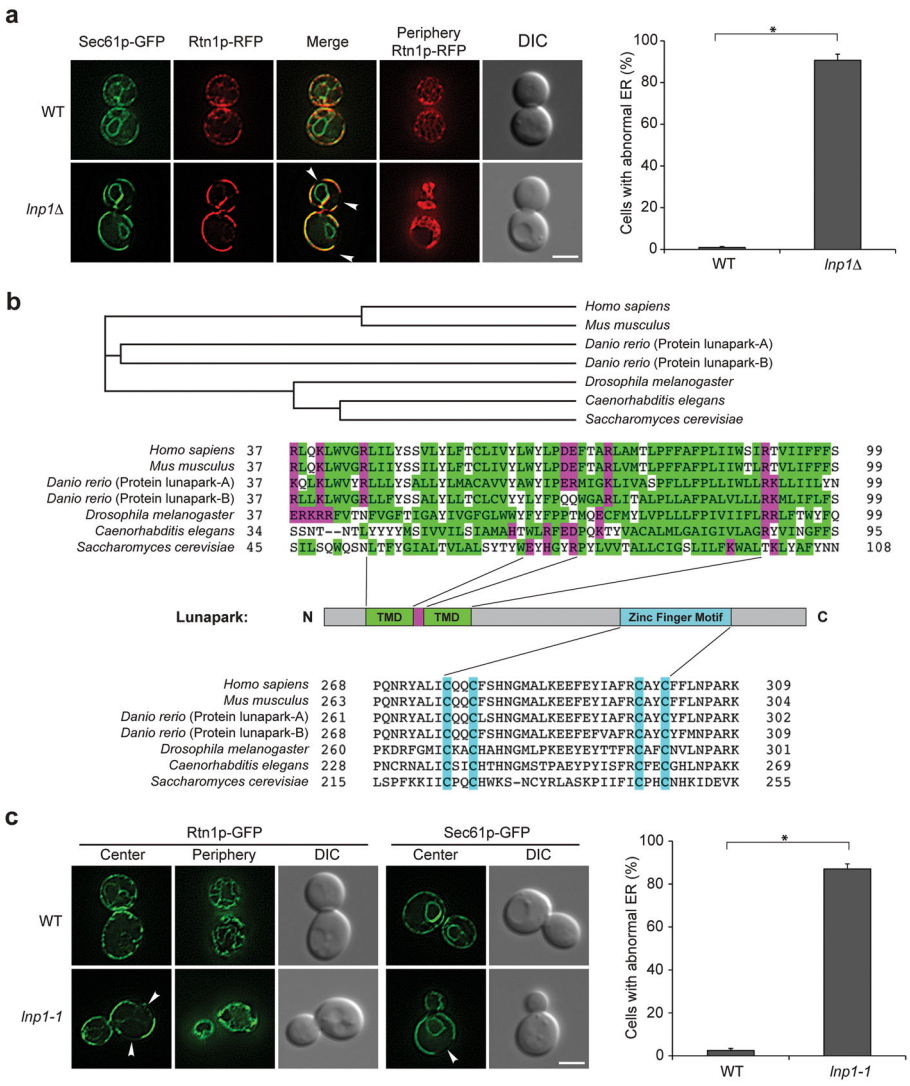

Figure 1. Cortical ER morphology is abnormal in the *lnp1* mutant

a, Yeast cells expressing Sec61p-GFP and Rtn1p-RFP (SFNY 2111, SFNY 2112) were grown to early log phase in YPD medium at 25°C. Subsequently, the cells were harvested and directly examined under the fluorescence microscope. The percentage of cells with abnormal ER morphology was quantified (right) from cells expressing Rtn1p-RFP. Error bars are S.E.M for three separate experiments, n=297 cells for wild type and n=258 cells for the *lnp1*Δ mutant. *P < 0.001 Student's t-test. **b**, Alignment of the transmembrane domain and zinc finger motif of the lunapark protein from yeast to man. Hydrophobic amino acids are shown in green and charged amino acids in purple. The four cysteines that form an atypical Cys4 type zinc finger motif are highlighted in blue. The beginning and end of the transmembrane domains are marked on the *Saccharomyces cerevisiae* sequence. **c**, The zinc finger motif plays a role in ER morphology. Same as **a** only the following number of cells was quantitated (right), n = 334, wild type (SFNY 2088, SFNY 2094); n = 391, *lnp1-1*(SFNY 2116, SFNY 2120). Error bars represent S.E.M for three separate experiments

*P < 0.001 Student's t-test. The arrowheads in **a** and **c** point to areas of the cortex that lack cortical ER. The scale bar is 3 μm.

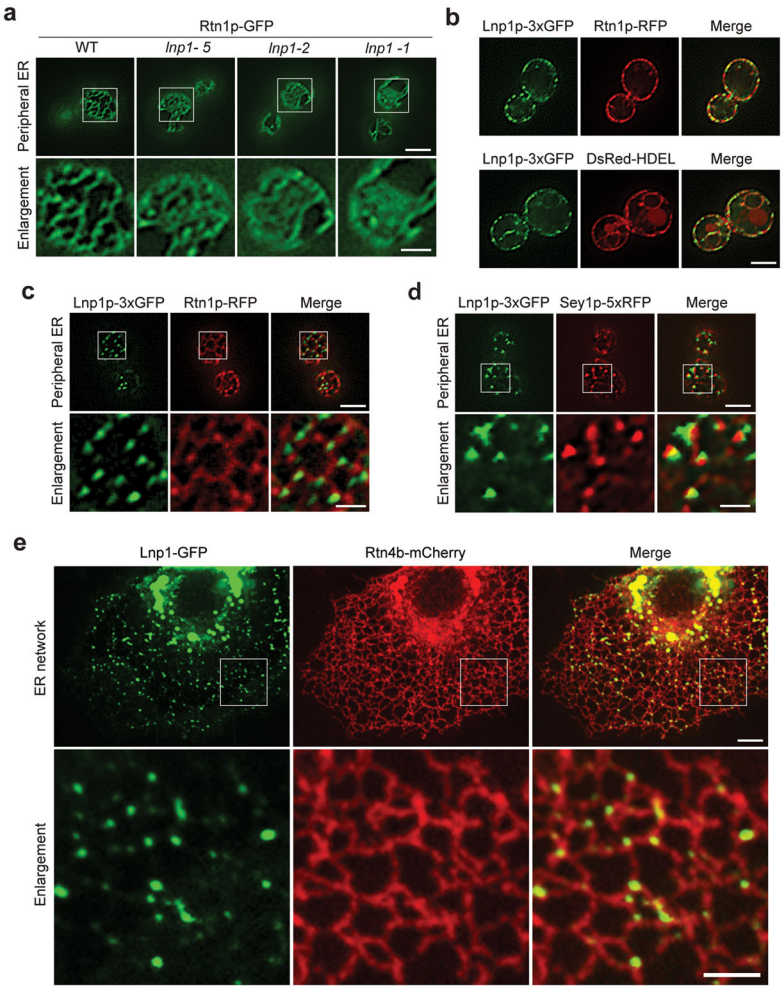

Figure 2. Lnp1p resides at three way junctions

a, The ER network collapses in *lnp1* mutant cells. Wild type (SFNY 2088) and mutant cells expressing Rtn1p-GFP were grown to early log phase in YPD medium at 25°C and harvested. Live cells were directly examined under the fluorescence microscope and the images were deconvolved. The boxed area is enlarged in the bottom panel. For the *lnp1-1* mutant (SFNY 2116), the zinc finger mutations are C223A C226A C244A C247A. For the *lnp1-5* mutant (SFNY 2142), the zinc finger mutation is C223A. For the *lnp1-2* mutant (SFNY 2113), the zinc finger mutations are C223A C226A. **b**, Lnp1p-3xGFP is present on puncta that line the tubular ER. Cells expressing Lnp1p-3xGFP and Rtn1p-RFP (SFNY 2093, top) or Lnp1p-3xGFP and DsRed-HDEL (SFNY 2100, bottom) were grown to early log phase in YPD medium at 25°C, harvested and the live cells were directly examined under the fluorescence microscope. **c**, Lnp1p-3xGFP localizes to three way junctions. Cells expressing Lnp1p-3xGFP and Rtn1p-RFP (SFNY 2093) were grown and examined as in **a**. The boxed area is enlarged in the bottom panel. **d**, Lnp1p-3xGFP partially overlaps or is adjacent to Sey1p-RFP at three way junctions. Yeast cells expressing Lnp1p-3xGFP and Sey1p-RFP (SFNY 2143) were grown and examined as in **a. e**, Human Lnp1-GFP localizes to the three way junctions of the ER marked by Rtn4b-mCherry in COS-7 cells. The boxed area is enlarged in the bottom panel. Scale bars in **b** and the peripheral images in **a**, **c**, and **d**

are 3 μm. Scale bars in the enlarged images in **a**, **c**, and **d** are 1 μm. Scale bar in **e** (top) is 10 μm, and the scale bar in the enlarged images in **e** (bottom) is 5 μm.

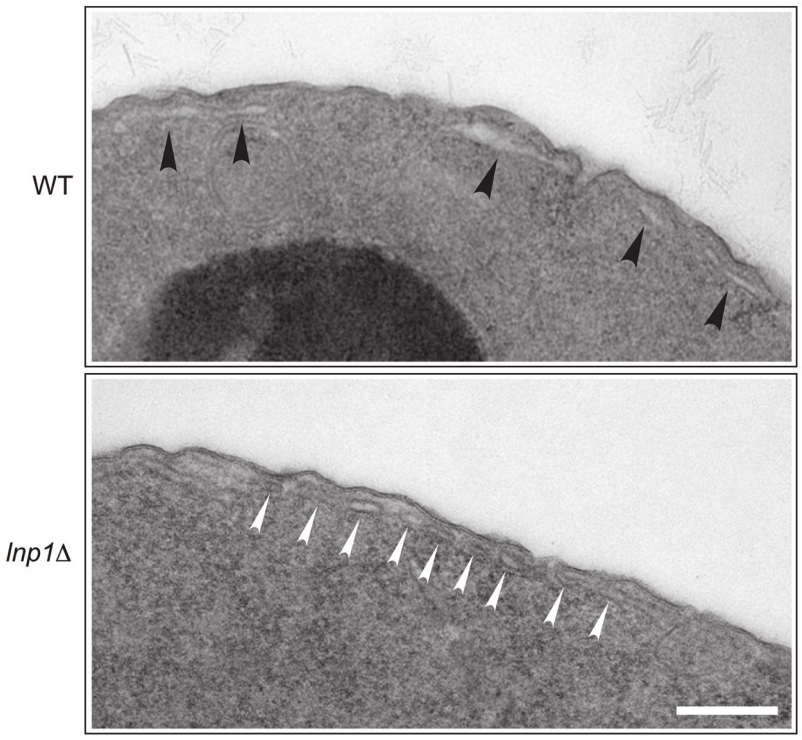

Figure 3. The cortical ER is highly reticulated in the *lnp1*Δ mutant

Yeast cells were grown, harvested and thin section analysis was performed as described in the **Methods**. In the cross section view, the arrows point to segments of ER in wild type (black arrowheads) and *lnp1*Δ mutant cells (white arrowheads). Scale bar is 200 nm.

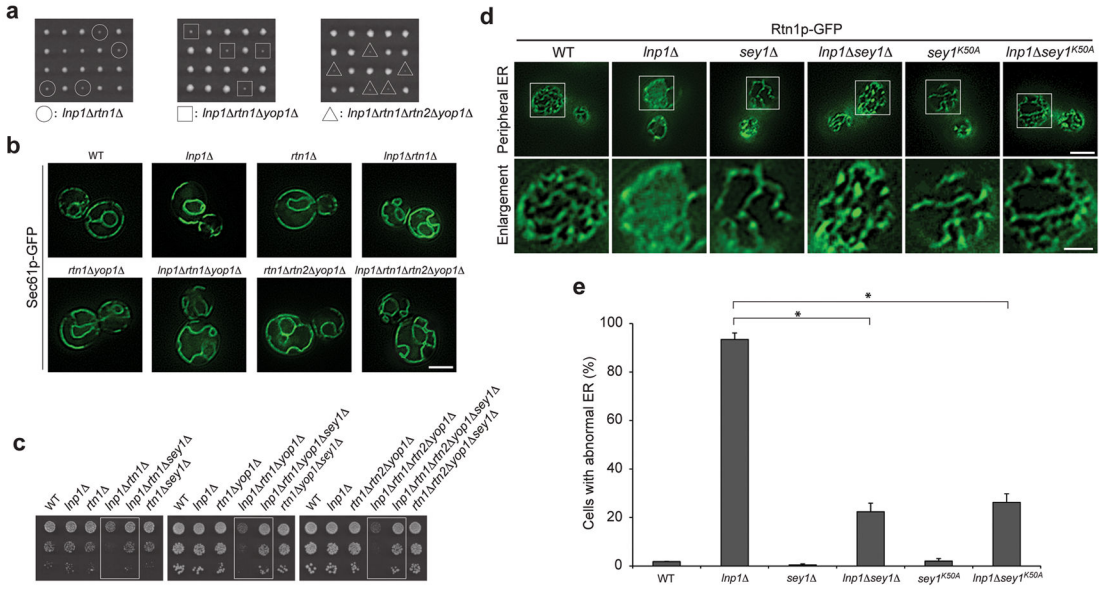

Figure 4. Lnp1p acts synergistically with the reticulons and Yop1p, but antagonistically with Sey1p

a, Lnp1p acts synergistically with the reticulons and Yop1p. Diploid *lnp1Δ/LNP1 rtn1Δ/RTN1*, *lnp1Δ/LNP1 rtn1Δ/RTN1 yop1Δ/yop1Δ*, and *lnp1Δ/LNP1 rtn1Δ/RTN1 rtn2Δ/rtn2Δ yop1Δ/yop1Δ* yeast cells were sporulated, dissected on YPD plates and the meiotic products were incubated for 3–5 days at 25°C. The *lnp1Δrtn1Δ* double mutant cells are marked with a white circle. The *lnp1Δrtn1Δ yop1Δ* triple mutant cells are marked with white squares. The *lnp1Δrtn1Δrtn2Δyop1Δ* quadruple mutant cells are marked with white triangles. **b**, Yeast cells expressing Sec61p-GFP (SFNY 2094, SFNY 2269, SFNY 2271, SFNY 2095, SFNY 2098, SFNY 2105, SFNY 2106, SFNY 2123) were grown to early log phase in YPD medium at 25°C, harvested and the livecells were directly examined under the fluorescence microscope. **c**, Lnp1p acts antagonistically with Sey1p.Yeast cells were grown to early stationary phase in YPD medium at 25°C, serially diluted and spotted on YPD plates. The plates were then incubated for 3–4 days at 25°C. The double, triple, quadruple, and quintuple mutant combinations examined in Fig. S3 are marked in white boxes. **d**, Loss of the GTPase activity of Sey1p is sufficient to suppress the ER morphology defect in the *lnp1Δ* mutant. Yeast cells expressing Rtn1p-GFP (SFNY 2088, SFNY 2090, SFNY 2126, SFNY 2128, SFNY 2147, SFNY 2148) were grown to early log phase in YPD medium at 25°C, harvested and the livecells were directly examined under the fluorescence microscope. Note that in our strain background *sey1Δ* has a more pronounced ER defect than previously reported [6]. The loss of Yop1p does not enhance the phenotype we see. **e**, Quantitation of the data in **d**. The percentage of cells with abnormal ER morphology was determined and the number of cells quantitated is listed below. Error bars represent S.E.M. for three separate experiments, n = 277 wild type; n = 298 *lnp1Δ*; n= 229 *sey1Δ*; n = 278 *lnp1Δsey1Δ*; n = 172 *sey1*^{K50A}; n = 333 *lnp1Δsey1*^{K50A}. *P < 0.001 Student's t-test. The scale bars in **b** and peripheral image in **d** are 3 μm. The scale bar in the enlarged images is 1 μm.

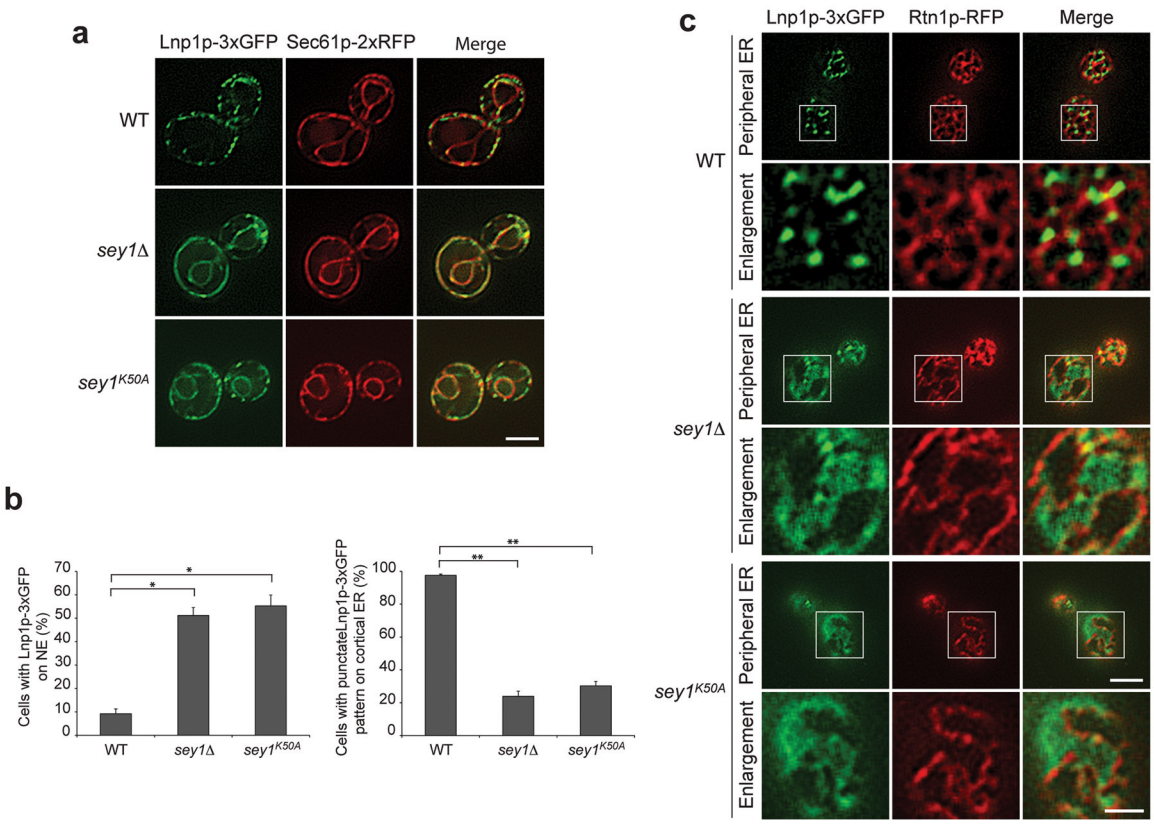

Figure 5. The GTPase activity of Sey1p retains Lnp1p at three way junctions

a, Yeast cells expressing Lnp1p-3xGFP and Sec61p-2xRFP (SFNY 2109, SFNY 2149, SFNY 2272) were grown to early log phase in YPD medium at 25°C, harvested and the live cells were examined directly under the fluorescence microscope. **b**, Left, quantitation of the nuclear envelope (NE) pattern of Lnp1p-3xGFP in wild type and *sey1* mutants. The number of cells examined is listed below. Error bars represent S.E.M. for three separate experiments, n = 296 wild type; n = 288 *sey1*Δ; n = 281 *sey1*^{K50A}. *P < 0.001 Student's t-test. Right, the percentage of cells in which Lnp1p-3xGFP is in a punctate cortical ER pattern was quantitated. The number of cells examined is listed below. Error bars represent S.E.M. for three separate experiments, n = 348 wild type; n = 336 *sey1*Δ; n = 243 *sey1*^{K50A}. **P < 0.0001 Student's t-test. **c**, Yeast cells expressing Lnp1p-3xGFP and Rtn1p-RFP (SFNY 2093, SFNY 2133, SFNY2146) were grown to early log phase in YPD medium at 25°C, harvested and the live cells were examined as above. The scale bars in **a** and peripheral images in **c** are 3 μm. The scale bar in the enlarged images is 1 μm.

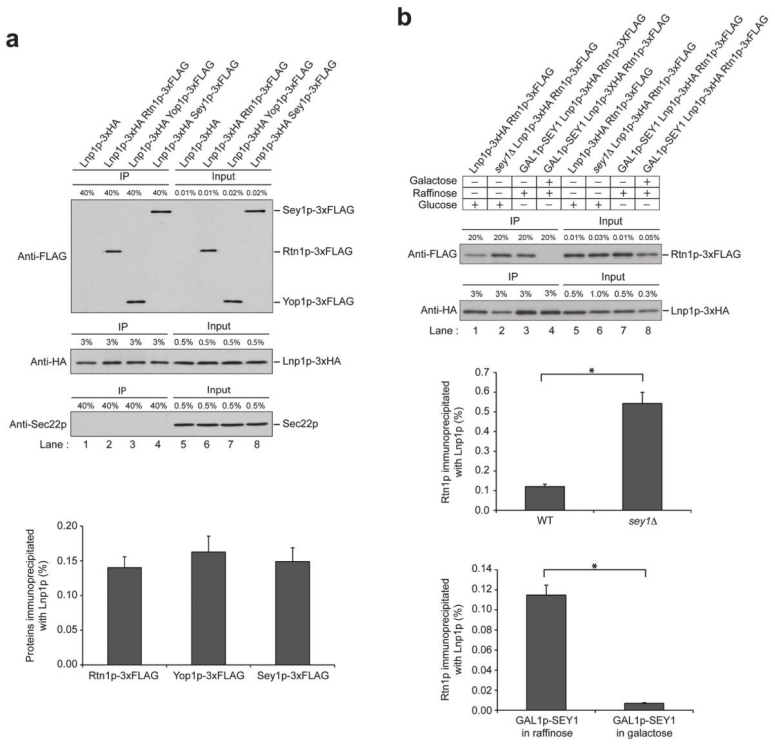

Figure 6. Sey1p regulates the interaction of Lnp1p with Rtn1p

a, Lnp1p interacts with Rtn1p, Yop1p and Sey1p. Yeast lysates were prepared from cells expressing either Lnp1p-3xHA and Rtn1p-3xFLAG (SFNY 2102), Lnp1p-3xHA and Yop1p-3xFLAG (SFNY 2103), or Lnp1p-3xHA and Sey1p-3xFLAG (SFNY 2104). Lysates were immunoprecipitated with anti-HA antibody and analyzed by western blot analysis using anti-FLAG, anti-HA and anti-Sec22p antibodies. Quantitation of the immunoprecipitates is shown on the bottom. Error bars represent S.D., n=3 **b**, Yeast lysates were prepared from cells expressing Lnp1p-3xHA and Rtn1p-3xFLAG when Sey1p was either absent or overexpressed (SFNY 2132, SFNY 2131). Overexpression of Sey1p was induced in YP medium with 0.1% galactose. Lysates were immunoprecipitated with anti-HA antibody and western blot analysis was performed using anti-FLAG antibody. The percent of the immunoprecipitate (IP) and lysate (Input) loaded on the gel is indicated at the top of each lane. Quantitation of the immunoprecipitates is shown on the bottom. Error bars represent S.E.M., n=3. *P < 0.02 Student's t-test.

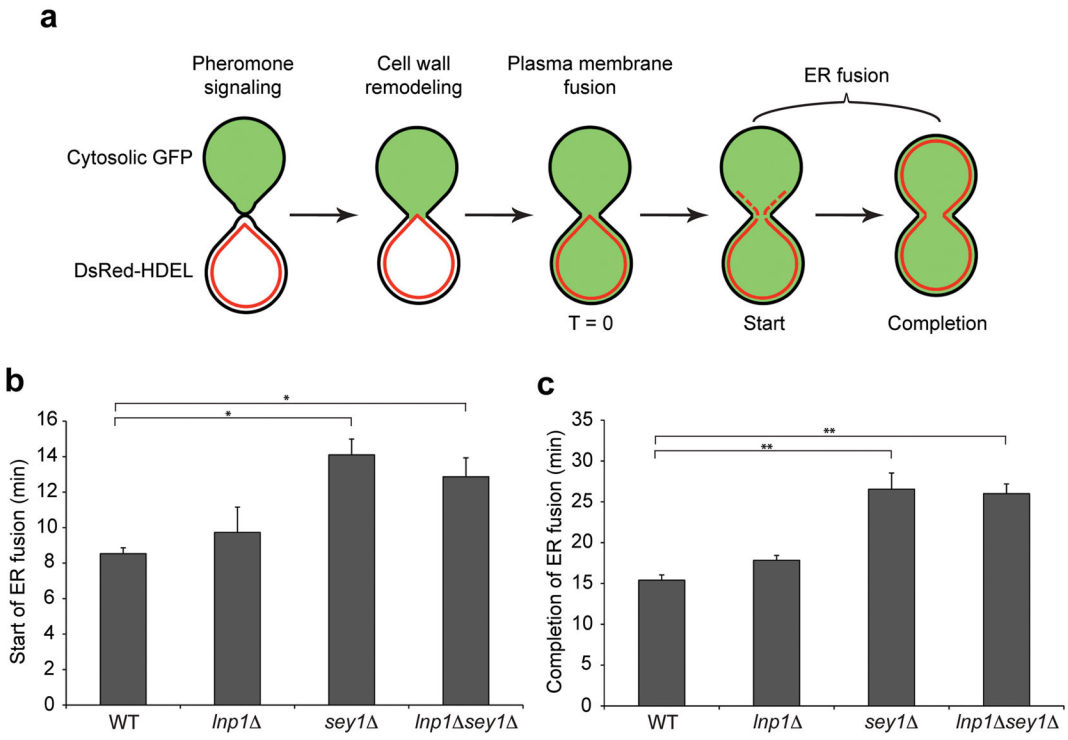

Figure 7. The *sey1*Δ mutant exhibits a delay in cortical ER fusion that is not suppressed by the loss of Lnp1p

a, Haploid MAT*a* and MAT*α* yeast cells expressing cytosolic GFP or DsRed-HDEL were grown to log phase in SC media. An equal number of cells of each mating type were mixed, incubated on an agarose pad of SC medium at 25°C for 40–60 min and cortical ER fusion was observed by fluorescence microscopy. Cell-cell fusion was marked by cytosolic GFP mixing (T=0). **b**, Quantitation of the time from T=0 to the start of ER fusion, marked by the appearance of DsRed-HDEL in the GFP expressing cell. Error bars represent S.E.M. for three separate experiments, n = 40 wild type; n = 40 *lnp1*Δ; n= 50 *sey1*Δ; n = 49 *lnp1*Δ*sey1*Δ. *P < 0.02 Student's t-test. **c**, Quantitation of the time it takes to complete ER fusion, from T=0 to the time it takes DsRed-HDEL to evenly spread into the GFP expressing cell. Error bars represent S.E.M. for three separate experiments, n = 40 wild type; n = 40 *lnp1*Δ; n= 50 *sey1*Δ; n = 49 *lnp1*Δ*sey1*Δ. **P < 0.01 Student's t-test.

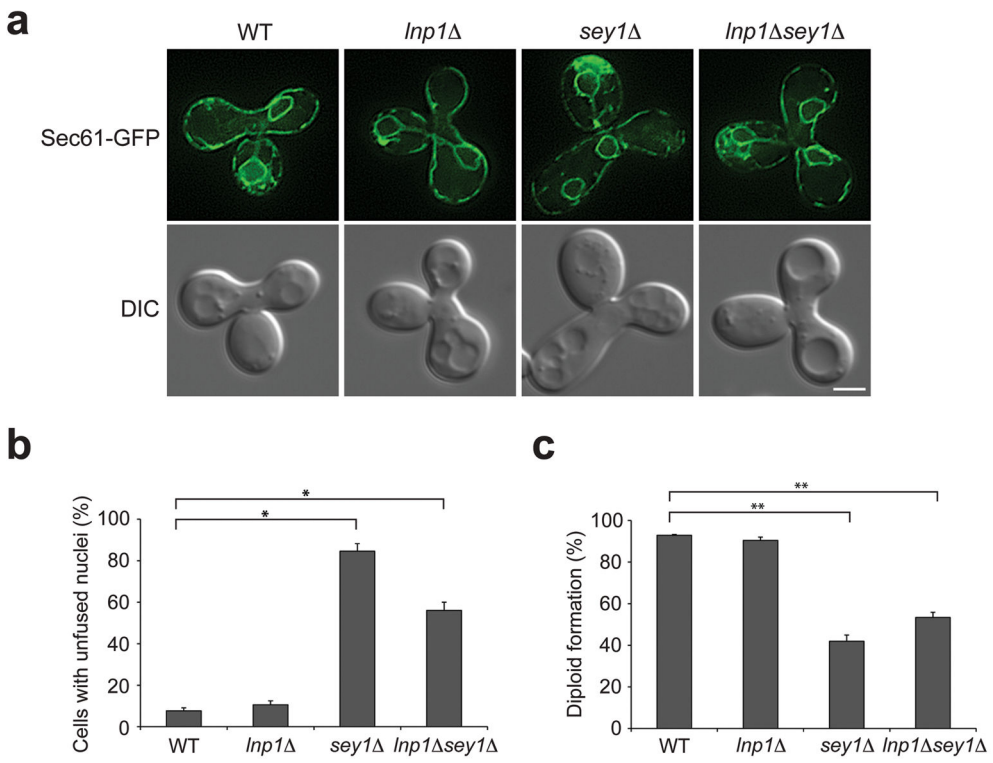

Figure 8. The *sey1*Δ mutant exhibits a defect in nuclear fusion that is not suppressed by the loss of Lnp1p

a, Haploid MAT*a* and MAT*α* yeast cells expressing Sec61p-GFP were grown to early stationary phase. Equal numbers of cells of each mating type were mixed, incubated at 25°C for 2–4 hr on a YPD plate and examined for nuclear fusion under the fluorescence microscope. **b**, Quantitation of the data in **a**. The number of cells examined is listed below. Error bars represent S.E.M. for three separate experiments, n = 65 wild type; n = 55 *lnp1*Δ; n= 38 *sey1*Δ; n = 48 *lnp1*Δ*sey1*Δ. *P < 0.01, Student's t-test. **c**, Same as **a** except zygotes were picked, transferred to a YPD plate and incubated for 4 days at 25°C. Cells were considered to be diploid if they sporulated and could no longer mate with MATa and MAT*α* tester strains. The number of cells examined is listed below. Error bars represent S.E.M., n = 85 wild type; n = 95 *lnp1*Δ; n= 123 *sey1*Δ; n = 127 *lnp1*Δ*sey1*Δ. **P < 0.005 Student's t-test. The scale bar is 3 *μ*m.